Asian Journal of Chemistry Vol. 22, No. 9 (2010), 7187-7196

Cycloaddition Reaction between Dibromovinylidene and Formaldehyde: A Density Functional Theory Study

GUO-LIANG DAI*, HUA YAN, AI-GUO ZHONG and CHUAN-FENG WANG
School of Pharmaceutical and Chemical Engineering,
Taizhou University, Linhai 317000, P.R. China
E-mail: daigl@tzc.edu.cn

The mechanism of the cycloaddition reaction between dibromovinylidene and formaldehyde has been characterized by density functional theory. All the stationary points were determined at the B3LYP/6-311++G** level of the theory. Single point CCSD(T)/6-311++G** calculation was used to get accurate energy. We have also calculated the changes of thermodynamic functions and the quality of kinetic properties for this reaction at different temperatures by using statistical thermodynamics method and transition-state theory. The results show that the present reaction has two major pathways. The first one brings about a three-membered ring product (P1) with a low energy barrier of 45.9 kJ/mol (14.6 kJ/mol relative to reactants). The latter one can generate a four-membered ring product P2, this is a spontaneous and great exothermic reaction. In view of dynamics and thermodynamics, it is between 500-1000 K that the major reaction may have not only the larger spontaneous tendency and equilibrium constant but also quicker reaction rate.

Key Words: DFT, Cycloaddition, Mechanism, Carbene.

INTRODUCTION

Due to the great importance in organic chemistry, the cycloaddition reaction has been widely used and got rapid development[1-6]. In order to better understanding the fundamental aspects of this kind of reactions, many attentions have been put to reveal the relevant mechanism[7-17]. As a kind of active intermediate, unsaturated carbene can provide simple and direct synthesis for small-ring, highly strained compounds, as well as those that are hardly synthesized through conventional ways[2]. Compared with the saturated carbenes, the study of unsaturated carbene is still at the initial stage, which is a new branch of carbene chemistry. One of the reasons may owe to the active character of unsaturated carbene, making it quite difficult to investigate the mechanism of cycloaddition reaction directly using experimental methods. In recent years, theoretical calculations have been employed to study the mechanism of cycloaddition reactions between unsaturated carbene and some π-bonded systems and proved to be very useful[8-17].

Because of the important application of the halogen-substituted carbene in medicine synthesis[18,19], in the present paper we choose dibromomethylene carbene and formaldehyde as model molecules to explore further the rules of the cycloaddition reaction between unsaturated carbene and the asymmetric-bonded compounds. The cycloaddition reaction mechanism was investigated and analyzed.

Recently, Chen *et al.*[20-22] pointed out that it is more important to investigate the effects of increased temperatures on a family of related parallel reactions. Therefore, further calculations of thermodynamic and kinetic properties with different temperatures have been performed in present study.

COMPUTATIONAL METHODS

The potential energy surface (PES) for the cycloaddition reaction between dibromovinylidene and formaldehyde has been considered in detail. We optimized all molecular geometries (reactants, intermediates, transition states and products) by employing the B3LYP density functional theory method. The harmonic vibration analyses were performed at the same level of theory for all optimized stationary points to determine their characters (minimum or first-order saddle point) and to evaluate the zero-point vibrational energies (ZPEs). To verify whether the located transition states connect the expected minima, intrinsic reaction coordinate (IRC) calculations were carried out for each transition state at the same level[23]. To obtain an accurate evaluation of the energy, the coupled cluster single-point calculations are performed using the B3LYP structures. All calculations in the present study were performed using the Gaussian 03 program[24].

Recently, the Erying transition state theory (TST)[25] with the Wigner correction was used to research the dynamic character of a reaction, through it one can obtain the most feasible range of reaction temperature, which has instructional value for further experiments. In this paper, according to thermodynamics and Erying transition state theory (TST) with the Wigner correction, we computed the change of thermodynamic functions and the reaction rate k.

$$k = g(k_bT/h)\exp(\Delta_r^{\neq}S_m^{\theta}/R - \Delta_r^{\neq}H_m^{\theta}/RT)$$

$$g = 1 + (h\nu^{\neq}/k_bT)^2/24,$$

$$A = g(k_bT/h)\exp(\Delta_r^{\neq}S_m^{\theta}/R)$$

here g represents Wigner correction factor, A is pre-exponential factor, k_b is boltzmann constant, $\Delta_r^{\neq}S_m^{\theta}$ and $\Delta_r^{\neq}H_m^{\theta}$ are activation entropy and activation enthalpy respectively.

RESULTS AND DISCUSSION

The optimized geometries of the stationary points over the potential energy surface (PES) for the reaction of dibromovinylidene with formaldehyde are depicted in Fig. 1. The relevant energies of various compounds in the reaction are listed in Table-1. The profiles of the PES are shown in Fig. 2. Fig. 3 is the frontier molecular orbital symmetry-adaption of $Br_2C=C$: and HCHO. The change of equilibrium constants (K) and rate constant (k) along reaction temperature T are drawn in Fig. 4.

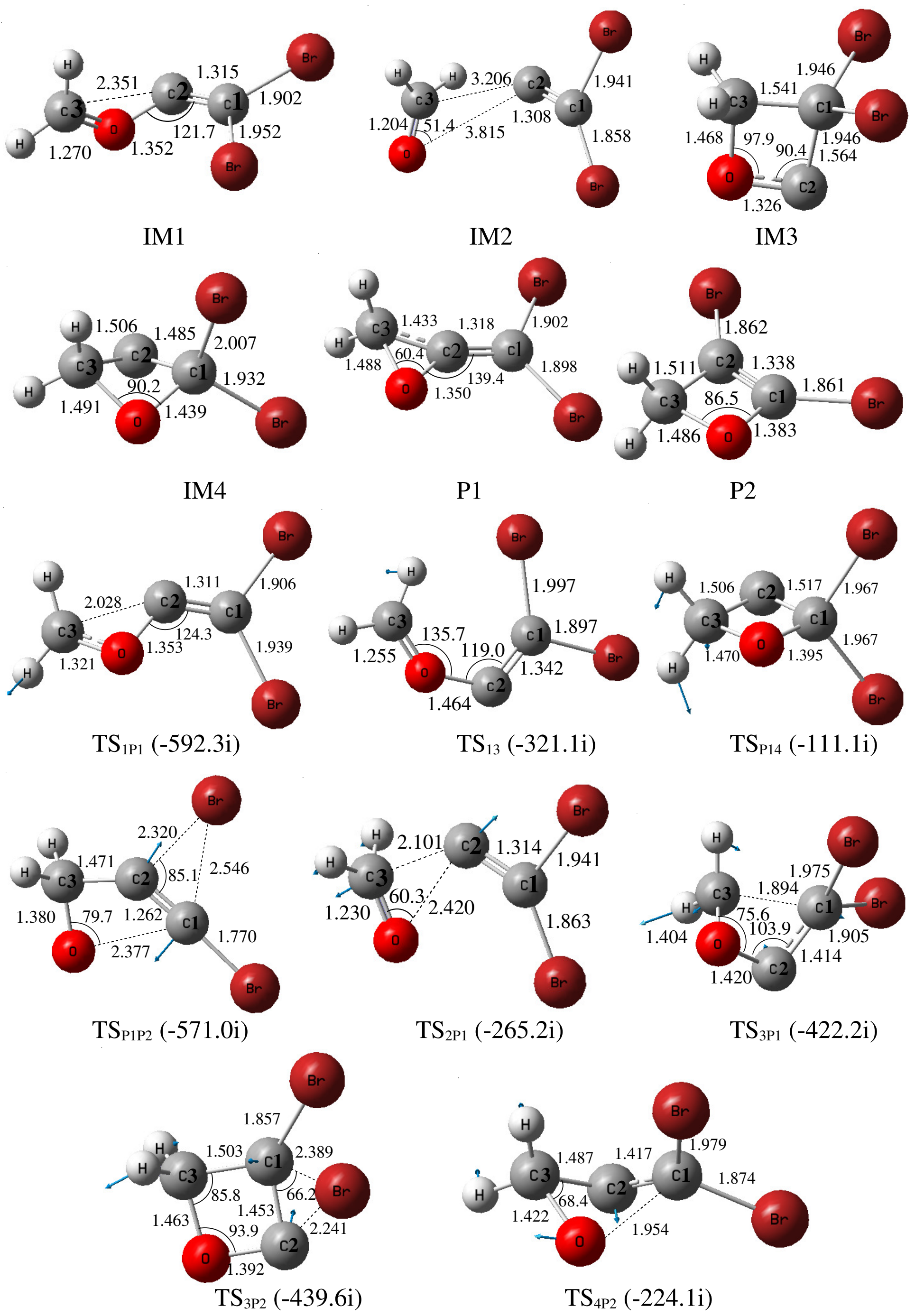

IM1 IM2 IM3

IM4 P1 P2

TS_{1P1} (-592.3i) TS_{13} (-321.1i) TS_{P14} (-111.1i)

TS_{P1P2} (-571.0i) TS_{2P1} (-265.2i) TS_{3P1} (-422.2i)

TS_{3P2} (-439.6i) TS_{4P2} (-224.1i)

Fig. 1. Optimized geometries for the various stationary points located on the potential energy surface (distances in angstroms, angles in degrees, the imaginary frequency of transition states are also listed)

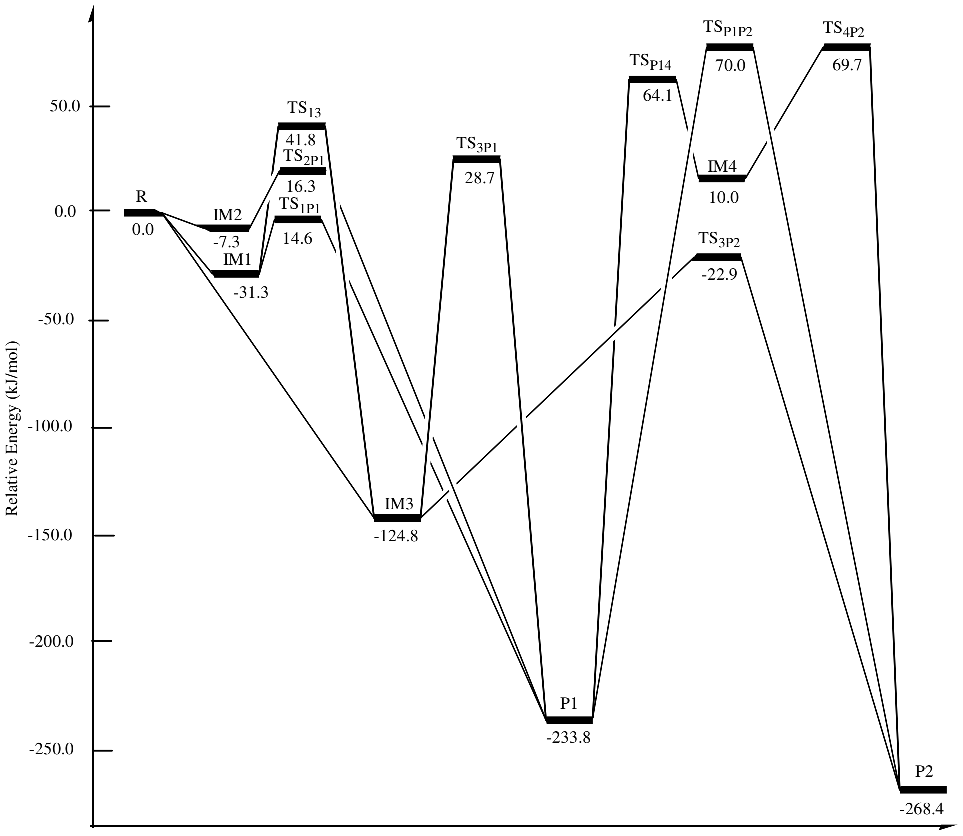

Fig. 2. Potential energy surface for the cycloaddition reaction between dibromovinylidene and formaldehyde with CCSD(T)/B3LYP/6-311++G**

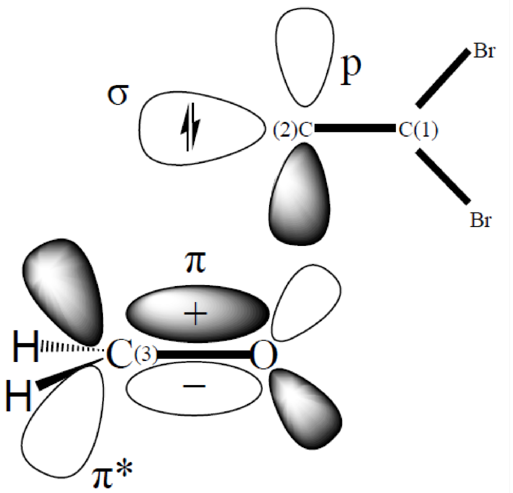

Fig. 3. Molecular orbital symmetry-adaption of dibromovinylidene and formaldehyde

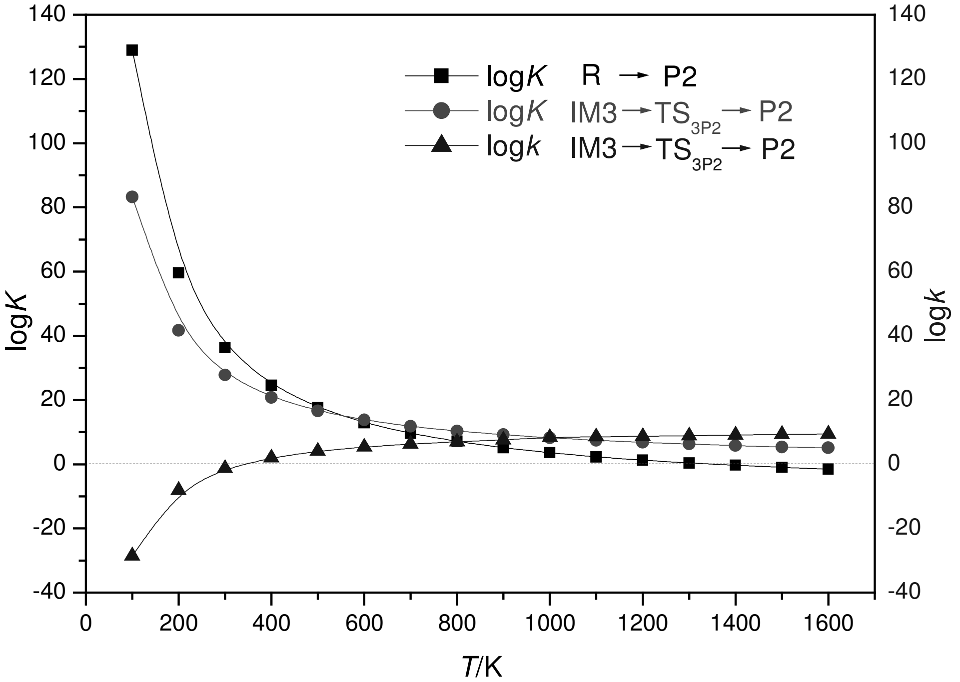

Fig. 4. Equilibrium constants (K) and rate constant (k) along reaction temperature T

TABLE-1
ENERGY OF VARIOUS COMPOUNDS IN THE REACTION (TOTAL ENERGY E_T, ZPE CORRECTIONS HAVE BEEN TAKEN INTO ACCOUNT, RELATIVE ENERGY E_R, ACTIVATING ENERGY FOR TRANSITION STATES $E^{\neq}$)

Species	B3LYP/6-311++G**			CCSD(T)/6-311++G**		
	E_T/Hartree	ZPE/Hartree	E_R/kJ mol^{-1}	E_T/Hartree	E_R/kJ mol^{-1}	$E^{\neq}$/kJ mol^{-1}
Reactants	-5338.865272	0.034206	0.0	-5335.1135349	0.0	–
IM1	-5338.880615	0.040093	-40.3	-5335.1254723	-31.3	–
IM2	-5338.866751	0.035116	-3.9	-5335.1163254	-7.3	–
IM3	-5338.904011	0.042030	-101.7	-5335.1610692	-124.8	–
IM4	-5338.854350	0.040174	28.7	-5335.1097413	10.0	–
P1	-5338.954788	0.042323	-235.0	-5335.2025665	-233.8	–
P2	-5338.964713	0.043427	-261.1	-5335.2157581	-268.4	–
TS_{1P1}	-5338.855452	0.039155	25.8	-5335.1079716	14.6	45.9
TS_{13}	-5338.856190	0.038436	23.8	-5335.0976318	41.8	93.5
TS_{3P1}	-5338.849437	0.038941	41.6	-5335.1025929	28.7	109.0
TS_{P14}	-5338.839686	0.039392	67.2	-5335.0891101	64.1	297.9
TS_{P1P2}	-5338.845245	0.038739	52.6	-5335.0868584	70.0	303.8
TS_{2P1}	-5338.859536	0.037093	15.1	-5335.1073397	16.3	23.6
TS_{3P2}	-5338.874101	0.040486	-23.2	-5335.1222741	-22.9	101.9
TS_{4P2}	-5338.838258	0.039294	70.9	-5335.0870022	69.7	59.7

Reactions lead to three-membered ring product P1

The first product generated from the reaction between dibromovinylidene and formaldehyde is a three-membered ring complex (P1). After calculation, we confirmed four different channels lead to P1 formation.

As shown in Fig. 2, the first reaction channel starts with the formation of an encounter complex IM1 ($^1A'$, C_1), which is -31.3 kJ/mol below the reactants. It should be pointed out that although numerous trials are taken to search for possible transition states that connect reactants and IM1, no such transition states are obtained. Obviously, the formation of IM1 is a barrier-free exothermic reaction. Starting from IM1, it can rearrange to form P1, which undergoes a formation of C-C bond *via* a transition state TS_{1P1} that is 45.9 kJ/mol above IM1. From Fig. 1, one can see the distance between two C atom in TS_{1P1} is shortened from 2.351 to 2.028 Å. This suggests that the C2-C3 bond is forming. TS_{1P1} is a typical 'early' transition state, as its structure is rather similar with that of intermediate IM1. Thus, it is understandable for TS_{1P1} to be only 45.9 kJ/mol above IM1, whereas 248.4 kJ/mol over P1. The unique imaginary frequency is 592.3i cm^{-1} and the corresponding normal mode corresponds to the formation of C2-C3 bond. For the three-membered ring product P1, its ground state is $^1A'$ with C_1 symmetry and it is 202.5 kJ/mol below the encounter complex IM1 and 233.8 kJ/mol more stable in energy than the reactants. As shown in Fig. 1, the C2-C3 bond length in P1 is shortened to 1.433 Å, which means this bond has formed.

Fig. 2 indicates that the second pathways of P1 formation consist of two steps: Starting from IM1, it can interconvert to IM3 *via* TS_{13}, facing a barrier height of 73.1 kJ/mol. IM3 is a four-membered ring intermediate with relative energy of -124.8 kJ/mol. The next step corresponds to the isomerization between IM3 and P1 *via* TS_{3P1}, the relative energy of this transition state is 28.7 kJ/mol, which is lower about 13.1 kJ/mol than that of the first step. Obviously, the first step, *i.e.* the process of IM3 formation is the rate-determining step along this path. Compared with the first P1 formation mechanism as discussed above, one can see that the energy of the transition state TS_{13} is 27.2 kJ/mol higher than that of the TS_{1P1}. According to the exponential law of reaction rate [$k = A\exp(-Ea/RT)$] the reaction rate from TS_{1P1} is approximately 1.6×10^5 times as fast as that from TS_{13} to IM3 at room temperature. Obviously, starting from encounter complex IM1, the reaction leads to P1 formation directly is the dominant channel instead of the IM3 formation through TS_{13}.

According to Fig. 2, one can see that the third pathway of P1 formation is completed by two steps. Similar with that of the IM1, the first step is also a barrier-free exothermic reaction of 7.3 kJ/mol, leading to an initial species IM2 formation. Then, this encounter species proceeds to form the addition product P1 through the transition state TS_{2P1}. This addition process is exothermic by 226.5 kJ/mol and has a barrier of 23.6 kJ/mol. From the frontier molecular orbital analysis as illustrated in Fig. 3, one can see that when two reactants approach each other, the unoccupied *p* orbital of the C2 end of dibromovinylidene overlaps with the π orbital of formaldehyde. At the same time, the lone pair σ electrons of dibromovinylidene overlap with the antibonding π* orbital which mainly located at the C3 end of formaldehyde. As a result, the π→p and σ→p* donor-acceptor bonds were formed, which may lead to the IM2 formation. As the distance between C2 and O atoms is too long (3.815 Å), the donor-acceptor bond of π→p between O and C2 is rather weak, resulting in the IM2 stores high energy. With reaction proceeding, IM2 may reduce its energy through shortening the distance between C2 and O atoms. As illustrated in Fig. 1, the C2-C3 bond distance in TS_{2P1} is shortened from 3.206 to 2.101 Å and the O-C2 bond is shortened by 1.395 Å. Compared with the first pathway, the relative energy of TS_{2P1} is only 1.7 kJ/mol higher than that of TS_{1P1}, so they can be considered as two competitive channels along the P1 formation process.

Next let's turn to the last P1 formation branch which starts from IM3. The direct [2+2] cycloaddition reaction between dibromovinylidene and formaldehyde can generate a four-membered ring intermediate IM3, which is a barrier-free process and this step can release a high amount of energy, 124.8 kJ/mol. However, similar with that of the second pathway, the next IM3→P1 isomerization process requires a high barrier of 153.5 kJ/mol, so this channel is of no importance and can be negligible in the mechanisms of P1 formation.

A comparison among the four different channels which generate P1, one can see that the rate-determining step of the first pathway has the lowest relative energy (14.6 kJ/mol), so we can predict that this pathway should be the major pathway lead to P1 formation.

Reactions lead to four-membered ring product P2

Next let us turn to the mechanism of P2 formation. As depicted in Fig. 2, the reaction generating a four-membered ring product P2 has three different pathways. The first possible product channel is the isomerization between P1 and P2 direct through transition state TS_{P1P2}, but the calculated energy barrier is as high as 303.8 kJ/mol, so this reaction channel is not feasible in kinetics. With respect to the second pathway, it can be described as: $P1 \rightarrow TS_{P14} \rightarrow IM4 \rightarrow TS_{4P2} \rightarrow P2$. From Fig. 1, one can see that in IM4, three carbon atoms and one oxygen atom have formed a twisted four-membered ring, this species stores very high energy. NBO analysis indicates that in IM4, the σ lone electron pair on C2 does not participate in the formation of bond, which results in the migration of bromine atom from C1 to C2, this may lead to the formation of P2. In the product P2, the C2 atom changes to sp^2 hybridization and forms σ bonds with its three neighbouring atoms, while simultaneously forming a π bond with C1. There are no longer any σ lone pair electrons on the C2, this is the main reason why the P2 is more stable. Nonetheless, this channel still involves significant barriers, especially in the second step, the relative energy of TS_{4P2} is as high as 69.7 kJ/mol. Therefore, this P2 formation mechanism is not preponderant also.

Fig. 2 gives the potential energy profiles of the third pathway about P2 formation. According to Fig. 2, this channel involves two steps: the first one is the formation of IM3. The second one corresponds to the isomerization of IM3 to P2 *via* a transition state TS_{3P2} with a relative low energy barrier of 101.9 kJ/mol. The relative energy of TS_{3P2} is only -22.9 kJ/mol, which is even lower than that of the reactants. Clearly, the third pathway should be the most feasible one lead to P2 formation and the whole reaction $R \rightarrow IM3 \rightarrow TS_{3P2} \rightarrow P2$ is a spontaneous process which can release about 264.4 kJ/mol energy. This reaction is even more feasible than that of P1 formation.

In summary, the dominant product channel in the reaction of dibromovinylidene with formaldehyde reaction may be determined straightforward according to the potential surface in Fig. 2. As the pathway of formation four-membered ring product P2 is barrier-free and this product channel is the most favoured thermodynamic. It should be unambiguous to deduce that this species is the dominant product of the title reaction.

Thermodynamics and kinetic characters of the reaction lead to P2

As illustrated in Fig. 2, the rate-determining step along the major product P2 formation channel is $IM3 \rightarrow TS_{3P2} \rightarrow P2$. In order to obtain detailed dynamics and thermodynamics characters of this reaction, according to the statistic thermodynamics and Eyring transition state theory with the Wigner correction, we investigated the change of thermodynamics function for two reactions of $R \rightarrow P2$ and $IM3 \rightarrow TS_{3P2} \rightarrow P2$ at 1.0 atm and wide temperature range of 100-1600 K. The equilibrium constants (K) and corresponding functions of these two reactions are listed in Tables 2 and 3, respectively. As it can be seen from Table-2, during the temperature range of 100-1600 K, the reaction $R \rightarrow P2$ is an exothermic process with entropy reducing and energetically spontaneous. In general, with the temperature dropping, the equilibrium constants (K) will increase greatly, especially at 100 K, this value reaches 7.53×10^{128}. Obviously, this reaction is an exothermic process, especially under the condition of low temperature. From Table-3, one can see that for the reaction $IM3 \rightarrow TS_{3P2} \rightarrow P2$, the proof factor of Wigner (g) is bigger under low temperature, which can correct the negative-windage caused by penetrating effect in Eyring transition state theory. Similar with that of the reaction $R \rightarrow P2$, the reaction $IM3 \rightarrow TS_{3P2} \rightarrow P2$ is entropy reducing and exothermic process during the temperature range of 100-1600 K. In addition, from the change of Gibbs free energy function ($\Delta_r^{\neq} G_m^{\theta}$) and rate constant (k), one can see that the trend and limit of this reaction are lessened along the temperature rising, whereas the reaction rate constant (k) enhancing rapidly. Obviously, under the condition of high temperature, the reaction $IM3 \rightarrow TS_{3P2} \rightarrow P2$ is excellent in dynamics. It is worth mentioning here that the change of pre-exponential factor (A) is small during the bound of temperature change, so it can be regarded as a constant which is independent of temperature.

TABLE-2
THERMODYNAMIC CHARACTERS OF REACTION R→P2

T (K)	ΔS^o (J K^{-1} mol^{-1})	ΔH^o (kJ mol^{-1})	ΔG^o (kJ mol^{-1})	K	T (K)	ΔS^o (J K^{-1} mol^{-1})	ΔH^o (kJ mol^{-1})	ΔG^o (kJ mol^{-1})	K
100	-176.276	-264.372	-246.744	7.53×10^{128}	900	-196.456	-265.233	-88.423	1.36×10^{5}
200	-193.594	-266.819	-228.100	3.71×10^{59}	1000	-195.121	-263.970	-68.849	3.95×10^{3}
300	-199.861	-268.331	-208.373	1.90×10^{36}	1100	-193.857	-262.642	-49.399	2.21×10^{2}
400	-201.711	-268.954	-188.270	3.86×10^{24}	1200	-192.661	-261.266	-30.073	2.04×10^{1}
500	-201.556	-268.872	-168.094	3.64×10^{17}	1300	-191.535	-259.854	-10.859	2.73×10^{0}
600	-200.556	-268.321	-147.987	7.65×10^{12}	1400	-190.460	-258.412	8.232	4.93×10^{-1}
700	-199.242	-267.462	-127.993	3.56×10^{9}	1500	-189.452	-256.950	27.228	1.13×10^{-1}
800	-197.840	-266.412	-108.140	1.15×10^{7}	1600	-188.493	-255.464	46.125	3.12×10^{-2}

TABLE-3
THERMODYNAMIC AND DYNAMIC
CHARACTERS OF REACTION IM3→TS_{3P2}→P2

T (K)	g	ΔS^o (J K^{-1} mol^{-1})	ΔH^o (kJ mol^{-1})	ΔG^o (kJ mol^{-1})	K	$\Delta_r^{\neq}S_m^{\theta}$ (J K^{-1} mol)	A	$\Delta_r^{\neq}H_m^{\theta}$ (kJ mol^{-1})	k (s^{-1})
100	2.668	0.833	-159.454	-159.537	2.17×10^{83}	-2.682	4.03×10^{12}	78.355	3.43×10^{-29}
200	1.417	-0.556	-159.657	-159.546	4.68×10^{41}	-4.954	3.25×10^{12}	78.022	7.50×10^{-9}
300	1.185	-1.331	-159.846	-159.447	5.80×10^{27}	-6.699	3.31×10^{12}	77.589	4.57×10^{-2}
400	1.104	-1.971	-159.909	-159.121	6.02×10^{20}	-8.196	3.43×10^{12}	77.066	1.10×10^{2}
500	1.067	-2.523	-160.316	-159.055	4.14×10^{16}	-9.502	3.54×10^{12}	76.481	1.15×10^{4}
600	1.046	-2.966	-160.562	-158.782	6.66×10^{13}	-10.657	3.63×10^{12}	75.843	2.51×10^{5}
700	1.034	-3.318	-160.788	-158.465	6.69×10^{11}	-11.694	3.69×10^{12}	75.173	2.22×10^{6}
800	1.026	-3.586	-160.988	-158.119	2.11×10^{10}	-12.631	3.74×10^{12}	74.475	1.12×10^{7}
900	1.021	-3.795	-161.164	-157.749	1.43×10^{9}	-13.468	3.79×10^{12}	73.758	3.93×10^{7}
1000	1.017	-3.954	-161.321	-157.367	1.66×10^{8}	-14.242	3.82×10^{12}	72.986	2.37×10^{8}
1100	1.0138	-4.084	-161.452	-156.960	2.84×10^{7}	-14.954	3.85×10^{12}	72.277	4.03×10^{8}
1200	1.0116	-4.184	-161.568	-156.547	6.52×10^{6}	-15.615	3.87×10^{12}	71.521	4.56×10^{8}
1300	1.0099	-4.268	-161.668	-156.120	1.88×10^{6}	-16.226	3.89×10^{12}	70.755	7.93×10^{8}
1400	1.0085	-4.330	-161.760	-155.698	6.45×10^{5}	-16.799	3.90×10^{12}	69.983	1.27×10^{9}
1500	1.0074	-4.385	-161.838	-155.261	2.55×10^{5}	-17.334	3.91×10^{12}	69.206	1.89×10^{9}
1600	1.0065	-4.435	-161.903	-154.807	1.13×10^{5}	-17.841	3.92×10^{12}	68.421	2.67×10^{9}

Fig. 4 is the logarithm profiles of K and k along the temperature coordinate. It is obvious that during the change of temperature (100-1000 K), both reaction R→P2 and IM3→TS_{3P2}→P2 have great equilibrium constants (K), whereas the rate constant (k) of the latter is rather small below 500 K. So, In view of thermodynamics and dynamics characters from Tables 2 and 3, Fig. 4, we consider that the present reaction should proceed between 500-1000 K, as it will not only have the larger spontaneous tendency and equilibrium constant but also quicker reaction rate.

Conclusion

Density functional calculations have been performed to investigate the reaction of dibromovinylidene and formaldehyde in the gas phrase. The potential surface energy of the cycloaddition reaction between dibromovinylidene and formaldehyde has been explored. The following conclusions can be drawn from the present calculations.

(1) This reaction has two major channels. The first one gives a three-membered ring product P1 through TS_{1P1}, the calculation relative energy of this transition state is 14.6 kJ/mol. For the second channel which leads to a four-membered ring product P2 formation, it is spontaneous and exothermic greatly about 268.4 kJ/mol. Obviously, P2 is the dominant product of this reaction.

(2) In view of dynamics and thermodynamics, it is between 500-1000 K that the reaction will have not only the larger spontaneous tendency and equilibrium constant but also quicker reaction rate.

ACKNOWLEDGMENT

This work was supported by the Zhejiang Provincial Natural Science Foundation of China under Grant No. Y4090387.

REFERENCES

1. P.J. Stang, *Acc. Chem. Res.*, **15**, 348 (1982).
2. P.J. Stang, *Chem. Rev.*, **78**, 383 (1978).
3. Y. Apeloig, M. Karni, P.J. Stang and D.P. Fox, *J. Am. Chem. Soc.*, **105**, 4781 (1983).
4. D.P. Fox, P.J. Stang, Y. Apeloig and M. Karni, *J. Am. Chem. Soc.*, **108**, 750 (1986).
5. K.N. Houk, N.G. Rondan, C. Santiago, C.J. Gallo, R.W. Gandour and G.W. Griffin, *J. Am. Chem. Soc.*, **102**, 1504 (1980).
6. K.N. Houk and N.G. Rondan, *Tetrahedron*, **41**, 1555 (1985).
7. A.E. Keating, S.R. Merrigan, D.A. Singleton and K.N. Houk, *J. Am. Chem. Soc.*, **121**, 3933 (1999).
8. X.H. Lu, Y.H. Xu, H.B. Yu and W.R. Wu, *J. Phys. Chem.*, **A109**, 6970 (2005).
9. X.H. Lu, H.B. Yu, W.R. Wu and Y.H. Xu, *Int. J. Quant. Chem.*, **107**, 451 (2007).
10. B. Lu, H.B.Yu and Y.H. Xu, *Chin. J. Chem.*, **24**, 307 (2006).
11. X.H. Lu and W.R. Wu, *Acta Chim. Sinica*, **61**, 1707 (2003).
12. X.H. Lu, L.M. Zhai, Y.X. Wang and C.B. Liu, *Acta Chim. Sinica*, **60**, 769 (2002).
13. X.H. Lu and Y.X. Wang, *J. Phys. Chem.*, **A107**, 7885 (2003).
14. J.P. Pezacki, P.D. Wood, T.A. Gadosy, J. Lusztyk and J. Warkentin, *J. Am. Chem. Soc.*, **120**, 8681 (1998).
15. M.D. Su and S.Y. Chu, *Eur. J. Chem.*, **6**, 3777 (2000).
16. X.H. Lu, W.R. Wu, H.B. Yu and Y.H. Xu, *Chin. Sci. Bull.*, **50**, 1693 (2005).
17. Z.F. Li, L.L. Lu, J.W. Kang and X.Q. Lu, *Chin. Sci. Bull.*, **52**, 880 (2007).
18. M. Garcia, C. Delcampo, E.F. Llama and J.V. Sinisterra, *J. Chem. Soc. Perkin. Trans. I*, 1771 (1995).
19. M. Mitani, Y. Kobayashi and K. Koyama, *J. Chem. Soc. Perkin. Trans. I*, 653 (1995).
20. X.Y. Chen, C.X. Zhao, Y. Ping and G.Z. Ju, *Int. J. Quant. Chem.*, **85**, 127 (2001).
21. X.Y. Chen, T. Wu, J. Peng, C. Li, T. Yao and G.Z. Ju, *Phys. Chem. Chem. Phys.*, **1**, 657 (1999).
22. X.Y. Chen, T. Wu, Q. Ju, J. Ma and G.Z. Ju, *Int. J. Quant. Chem.*, **73**, 417 (1999).
23. K. Fukui, *Acc. Chem. Res.*, **14**, 363 (1981).
24. M.J. Frisch, *et al.* Gaussian 03, Revision B04, Gaussian Inc., Pittsburgh PA (2003).
25. D.G. Truhlar, B.C. Garrett and S.J. Klppenstein, *J. Phys. Chem.*, **100**, 12771 (1996).

(*Received*: 29 January 2010; *Accepted*: 22 June 2010) AJC-8817